Water Research 89 (2016) 107–117

Contents lists available at ScienceDirect

Water Research

journal homepage: www.elsevier.com/locate/watres

Water quality modeling in the dead end sections of drinking water distribution networks

Ahmed A. Abokifa [a], Y. Jeffrey Yang [b], Cynthia S. Lo [a], Pratim Biswas [a, *]

[a] Department of Energy, Environmental and Chemical Engineering, Washington University in St. Louis, MO 63130, USA
[b] U.S. EPA, Office of Research and Development, National Risk Management Research Laboratory, Cincinnati, OH 45268, USA

ARTICLE INFO

Article history:
Received 24 June 2015
Received in revised form
8 October 2015
Accepted 8 November 2015
Available online 18 November 2015

Keywords:
Chlorine
Dead end pipe
Advection dispersion
Genetic algorithm
Stochastic demands
Spatial distribution
Correction factors

ABSTRACT

Dead-end sections of drinking water distribution networks are known to be problematic zones in terms of water quality degradation. Extended residence time due to water stagnation leads to rapid reduction of disinfectant residuals allowing the regrowth of microbial pathogens. Water quality models developed so far apply spatial aggregation and temporal averaging techniques for hydraulic parameters by assigning hourly averaged water demands to the main nodes of the network. Although this practice has generally resulted in minimal loss of accuracy for the predicted disinfectant concentrations in main water transmission lines, this is not the case for the peripheries of the distribution network. This study proposes a new approach for simulating disinfectant residuals in dead end pipes while accounting for both spatial and temporal variability in hydraulic and transport parameters. A stochastic demand generator was developed to represent residential water pulses based on a non-homogenous Poisson process. Dispersive solute transport was considered using highly dynamic dispersion rates. A genetic algorithm was used to calibrate the axial hydraulic profile of the dead-end pipe based on the different demand shares of the withdrawal nodes. A parametric sensitivity analysis was done to assess the model performance under variation of different simulation parameters. A group of Monte-Carlo ensembles was carried out to investigate the influence of spatial and temporal variations in flow demands on the simulation accuracy. A set of three correction factors were analytically derived to adjust residence time, dispersion rate and wall demand to overcome simulation error caused by spatial aggregation approximation. The current model results show better agreement with field-measured concentrations of conservative fluoride tracer and free chlorine disinfectant than the simulations of recent advection dispersion reaction models published in the literature. Accuracy of the simulated concentration profiles showed significant dependence on the spatial distribution of the flow demands compared to temporal variation.

1. Introduction

Disinfection is consistently applied as the final treatment step in typical drinking water treatment plants. All water utilities in the U.S. are required to maintain a residual disinfectant concentration throughout the distribution system to inhibit microbial recontamination of treated drinking water. Chlorine, which is the most commonly used disinfectant worldwide, is a highly reactive oxidant that reacts with a variety of materials in both the bulk water and at the pipe wall as it transports through the distribution system pipes. In the last three decades, extensive research work was devoted to develop water quality models that simulate chlorine transport and decay in water distribution systems (Grayman, 2006). In the early work done by Biswas et al. (1993), a generalized model for steady state chlorine consumption that accounts for axial convection and radial diffusion was developed. It was the first model to appropriately account for chlorine decay at the pipe wall in addition to the bulk liquid phase. Rossman et al. (1994) developed a film mass transfer approach to account for radial chlorine transport and further reaction at the pipe wall. This 1-D advection-reaction model was incorporated in the water quality simulation module of the well-known software package EPANET (Rossman,

Abbreviations: ADR, advection dispersion reaction; CHBP, Cherry Hill Brushy Plains; CV, coefficient of variation; CF, correction factor; GA, genetic algorithm; GEP, gene expression programming; MOC, method of characteristics; SCCRWA, South Central Connecticut Regional Water Authority; RMSD, root mean square deviation.

* Corresponding author.
E-mail addresses: ahmed.abokifa@wustl.edu (A.A. Abokifa), yang.jeff@epa.gov (Y.J. Yang), clo@wustl.edu (C.S. Lo), pbiswas@wustl.edu (P. Biswas).

http://dx.doi.org/10.1016/j.watres.2015.11.025

Nomenclature

A	amplitude of inlet concentration sine wave (mg/L)
a	pipe radius (in)
C	instantaneous disinfectant concentration in the dead end (mg/L)
C^*	dimensionless disinfectant concentration = C/C_0
C_0	pipe inlet concentration (mg/L)
CV_{rms}	coefficient of variation of the root mean square deviation
E	longitudinal dispersion coefficient (m^2/sec)
E_T	Taylor's dispersion coefficient (m^2/sec)
D	molecular diffusivity (m^2/sec)
D_x^*	inverse of the radial Peclet number
Da	Damkohler number = $K\tau_0$
d	pipe diameter (in)
f^*	pipe friction factor
$f(r)$	radial flow distribution parameter
K	overall first order decay rate constant (sec^{-1})
k_b	decay rate constant for bulk flow (sec^{-1})
k_w	wall decay constant (m/sec)
k_f	mass transfer coefficient (m/sec)
L	pipe length (ft)
λ	period of the inlet concentration sine wave (hr)
N_{seg}	no. of withdrawal points along the axis of the dead end pipe
N_{meas}	No. of field measurements
Pe	axial Peclet number = uL/E
Q_b	base flow demand (L/hr)
R_w	overall wall demand (sec^{-1})
Re	Reynolds number
r	radial space coordinate (m)
r_h	pipe hydraulic mean radius (m)
τ_0	characteristic residence time (sec)
t	time (sec)
t_0	Lagrangian time scale = $a^2/16D$ (sec)
t^*	dimensionless time = t/τ_0;
u	average flow velocity in the pipe (m/sec)
W_d	wall demand parameter (m/sec)
x	axial space coordinate (m)
x^*	dimensionless axial distance = x/L

2000) which is widely used by water utilities worldwide. Although EPANET was able to accurately predict the field observed disinfectant concentrations for the water transmission mains, this was not the case for secondary branch pipes, the so called “dead-ends” at perimeters of a distribution system, where laminar flow conditions prevailed.

Distribution dead-end mains are characterized by intermittent low flow velocities and frequent stagnation times. They are well known problematic locations for the long and excessive residence times, leading to rapid water quality deterioration, disinfectant residuals disappearance and high potential for bacterial regrowth (Barbeau et al., 2005; Galvin, 2011). Few researchers gave special attention to water quality modeling in dead-ends, although they “often comprise 25% or more of the total infrastructure in a distribution system and tend to service a high percentage of the residential consumer base” as mentioned by Tzatchkov et al. (2002) based on the study of Buchberger and Lee (1999). For example, the Cherry Hill/Brushy (CHBP) plains water distribution network in New Haven, Connecticut has 32 dead-end links compared to 21 main trunk links out of total 103 pipes (Nilsson et al., 2005). Axworthy and Karney (1996) were the first to shed the light on the importance of considering dispersive transport in low flow velocity pipes as the advective transport models either would under- or over-predict the actual concentrations. Following this earlier work, several studies developed numerical 2-D convection-diffusion-reaction or 1-D advection-dispersion-reaction (ADR) models that efficiently simulate water quality under low flow conditions (Ozdemir and Ger, 1999, 1998; Islam and Chaudhry, 1998; Tzatchkov et al., 2002; Ozdemir and Ucak, 2002; Li et al., 2006; Basha and Malaeb, 2007). Spatial averaging of hydraulic parameters was employed in all these models by lumping multiple water uses into a single demand point assigned to a specified node on the network grid. For main water arteries, spatial aggregation is a good approximation because the ratio of the “on-pipe” demands compared to flows transmitted to downstream nodes is relatively small. However, this is not a good approximation for dead-ends, where all water demands are being directly withdrawn from the pipe at different spatial locations as shown in (Fig. 1-a). Applying spatial aggregation to dead ends will consistently overestimate the

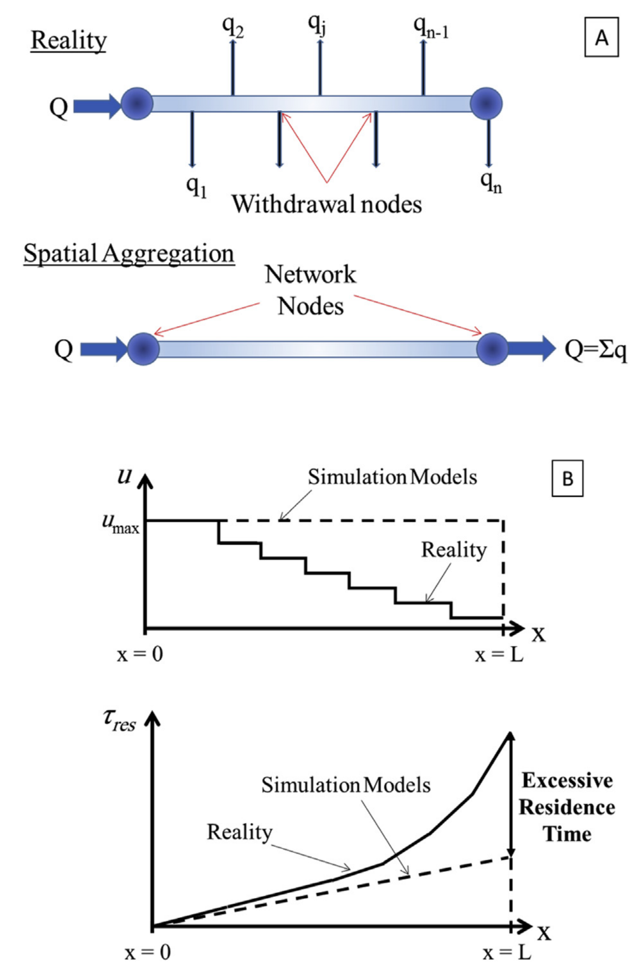

Fig. 1. **(A)** Spatial aggregation of flow demands compared to reality; **(B)** Over and under-estimation of average flow velocity (u) and residence time (τ_{res}) due to spatial averaging approximation.

average flow velocity at different pipe locations and under-predict the actual residence time (Fig. 1-b). The later will cause the simulated disinfectant concentrations to be systematically over-predicted (Tzatchkov et al., 2002; Li, 2006), or a higher wall demand coefficient would be required to fit field measured concentrations (Biswas et al., 1993; Yeh et al., 2008). The first study to address water distribution network dead-ends was done by Buchberger and Wu (1995). They generated the realistic spatial and temporal distributions of the flow rate and the corresponding Reynolds number at different sections along the dead end, but their hydraulic model was not coupled with a water quality simulator.

The primary objective of this study is to develop a realistic modeling approach to simulate water quality in dead ends while considering both temporal variation and spatial distribution of flow demands and the subsequent variability in transport parameters. The new model (Washington University Dead End Simulator – WUDESIM), is coupled with a stochastic demand generator based on a nonhomogeneous Poisson process to simulate residential water demand pulses on fine time scales. The model uses a genetic algorithm based optimization technique for calibrating the hydraulic profile of the dead end. The model is then applied to assess the effect of the uncertainty in the spatial distribution of water demands on the simulation accuracy using a Monte-Carlo simulation approach. A set of correction factors are analytically derived to correct the spatial aggregation approximation in simplified ADR models at low computational cost.

2. Methodology

2.1. Mathematical background

The solute transport in a dead end pipe can be appropriately modeled by a dynamic 2-D convection-diffusion equation in cylindrical coordinates to represent the mass balance on the disinfectant concentration $C(x,r,t)$, which can be written as (Biswas et al., 1993):

$$\frac{\partial C}{\partial t} = -\frac{\partial}{\partial x}(uf(r)C) + \frac{\partial}{\partial x}\left(D\frac{\partial C}{\partial x}\right) + \frac{1}{r}\frac{\partial}{\partial r}\left(rD\frac{\partial C}{\partial r}\right) - k_b C \tag{1}$$

where, x & r are the axial and radial spatial coordinates, respectively (m); t is the time (sec); u is the average flow velocity in the pipe (m/sec); $f(r)$ is the radial flow distribution parameter; D is the molecular diffusivity of solute in water (m^2/sec); and k_b is the first order decay rate constant in the bulk phase (sec^{-1}). The chlorine consumption at the pipe wall could be simulated by imposing a Robin type boundary condition for instant chlorine exhaustion at the wall ($r = a$, $D\partial C/\partial r + W_d C = 0$) where, a is the pipe radius (m), W_d is the wall demand parameter (m/sec). This boundary condition only applies to pipes with fast chlorine reaction at the wall, while for thicker pipe scales with significant biofilm thickness, a two layer mass transfer approach would be more appropriate.

The numerical solutions for the dynamic 2-D convection-diffusion equation are typically computationally intensive. Previous researchers treated this by either removing the time dependence represented by the accumulation term and then solving a steady state 2-D equation, or reducing the model to an unsteady 1-D advection-dispersion model to preserve the dynamic behavior of solute transport in water distribution systems. The latter approach was implemented in this study, and (Eq. (1)) simplifies to:

$$\frac{\partial C}{\partial t} = -u\frac{\partial C}{\partial x} + E\frac{\partial^2 C}{\partial x^2} - KC \tag{2}$$

where, E is the effective longitudinal dispersion coefficient (m^2/sec), K is the overall lumped first order decay constant (sec^{-1}) that accounts for disinfectant consumption both in the bulk phase and at the pipe wall. (Rossman et al., 1994) used a lumped mass-transfer coefficient to account for the radial transport of solute and further first order reaction at the pipe wall analogous to film models for heat transfer: $K = k_b + R_w$ where, k_b is the bulk demand coefficient (sec^{-1}); R_w is the overall wall demand: $R_w = k_w k_f / r_h(k_w + k_f)$; k_w is the wall decay constant (m/sec); k_f is the mass transfer coefficient (m/sec); and r_h is the pipe hydraulic mean radius (m). Removing the dispersion term in (Eq. (2)) gives the 1-D advection-reaction equation incorprated in EPANET.

The 1-D ADR equation in the dimensionless form is:

$$\frac{\partial C^*}{\partial t^*} = -\frac{\partial C^*}{\partial x^*} + \frac{1}{Pe}\frac{\partial^2 C^*}{\partial x^{*2}} - Da\, C^* \tag{3}$$

where, C^* is the dimensionless concentration $= C/C_0$; t^* is the dimensionless time $= t/\tau_0$; x^* is the dimensionless distance $= x/L$; Pe is the axial Peclet number $= uL/E$; and Da is the Damkohler number $= K\tau_0$. C_0 is a reference concentration usually taken as the inlet concentration (mg/L); while τ_0 is the characteristic residence time $= L/u$ (sec); and L is the pipe length (m).

The main concern that arises from reducing the 2-D model into a 1-D model is the error caused by neglecting the combined effects of radial molecular diffusion and the parabolic flow velocity profile in the radial direction ($f(r) = 2[1-(r/a)^2]$ for fully developed laminar flow). The incorporation of an appropriate dispersion coefficient is crucial for the success of such approximation. The classical work by Taylor (1953) was widely used in the literature, where the dispersion coefficient in the steady laminar flow can be simulated as:

$$E_T = \frac{a^2 u^2}{48D} \tag{4}$$

However, Taylor's formula only provides the ultimate value that the dispersion coefficient approaches after a certain initialization period has elapsed given by: $t > 0.5\frac{a^2}{D}$ which for a typical dead end pipe, with a 6-inch diameter, would be approximately twenty weeks for a solute with a molecular diffusivity in the order of 10^{-9} m^2/sec (e.g. chlorine). Given that extended stagnation periods are typically encountered in dead ends leading to a partial loss in the dispersion memory between demand pulses, the longitudinal dispersion in pulsating laminar flow will always be within the initialization period. Hence, the use of a highly dynamic time-evolving dispersion coefficient is essential to simulate the complex nature of flow demands in dead ends. In this study, the dynamic rates of dispersion developed by Lee (2004) for pulsating laminar flows are implemented where the instantaneous rate of dispersion is expressed as a dynamic weighted average of two factors: (i) the dispersion memory from previous pulses; and (ii) the nonlinear excitation from the current pulse. The instantaneous rate of dispersion during pulse (k) is given as:

$$E_k(t) = E_{k-1}(t_{k-1})\left(\frac{u_k}{u_{k-1}}\right)\exp\left(-\frac{t-t_{k-1}}{t_0}\right) + E_{T_k}\left[1-\exp\left(-\frac{t-t_{k-1}}{t_0}\right)\right] \tag{5}$$

where, E_{k-1} is the instantaneous dispersion coefficient for pulse ($k-1$); t_{k-1} is the ending time of pulse ($k-1$); E_{T_k} is the Taylor's dispersion coefficient for pulse (k); $t_0 = a^2/16D$ is a Lagrangian time scale. If the flow is intermittent so that pulse ($k-1$) is stagnant (i.e., $u_{k-1} = 0$); then the first term on the RHS should telescope to pulse ($k-2$). The time-averaged rate of dispersion during any pulse (k) is calculated as:

$$\overline{E}_k = \frac{1}{(t_k - t_{k-1})} \int_{t_{k-1}}^{t_k} E_k(t)dt \quad (6)$$

The present study is the first to use these highly dynamic dispersion rates, as this was made possible by coupling the water quality simulator with a stochastic demands generator that simulates random demand pulses on a second by second basis. The average flow velocities are generally low in dead end pipes where laminar conditions prevail and the solute transport is dominated by axial dispersion, as the values of *Pe* are generally small. However, large flow rates can also take place during peak demand hours where occasional transitional or turbulent conditions occur leading to advection dominated transport. In this model, longitudinal dispersion in the transitional and turbulent regimes (Re > 2300) was also considered using the empirical formula derived by Sattar, (2013) using gene expression programming (GEP):

$$D_{x*} = c_1 f^{*c_2} d^{c_3}/u \quad (7)$$

where, D_x^* is the inverse of the radial Peclet number; f^* is the pipe friction factor (Taylor, 1954); d is the pipe diameter; $c_1 = 219$; $c_2 = 2.82$; and $c_3 = -0.82$. The formula (GEP3) was chosen as it showed reasonable description of the experimental data for Reynolds numbers in the range (2300 < Re < 10,000). The classical formula developed by (Taylor, 1954) and widely applied in water distribution models wasn't implemented in this study as it is only valid under highly turbulent regimes (Re > 20,000) (Ekambara and Joshi, 2003). A situation that is highly unlikely to take place in dead ends where flow regimes are largely laminar with only occasional transitional to early turbulent flows.

Because of the spatial variation in flow velocity at different axial locations, transport and reaction parameters are not only considered as functions of time, but axial coordinate as well, i.e.: $u = u(x,t)$; $E = E(x,t)$; and, $K = K(x,t)$. This is simulated by splitting the dead end into a specified number of sections of variable lengths based on the locations of the draw off points (Fig. 1-a). The flow velocity decreases in the axial direction as a result of the withdrawals and the hydraulic profile is simply generated by mass continuity.

The initial condition is expressed by a given concentration profile in the pipe. The boundary conditions are expressed as follows:

(1) at $x = 0$; $C = C_0(t)$. The inlet node concentration is specified as a prescribed time series. This is the solute source (Fig. 1).
(2) at $x = L$; $\partial C/\partial x = 0$. The terminal node is described by a no-flux (free discharge) condition.

A special form of the original ADR equation is used to describe mass conservation at the withdrawal nodes due to the local discontinuity in the transport and reaction parameters *u*, *E* and *K*; further detail is given in Supplementary data section S-2.

2.2. Numerical approach

Analytical solutions for the ADR equation have only been developed for limited cases. For example, solutions developed by van Genuchten and Alves (1982) can only be applied to cases of steady flow where the dispersion coefficient and reaction rate are time independent. Although a wide range of numerical methods has been developed for solving the dynamic ADR, the mixed Eularian-Lagrangian numerical methods are particularly known to be efficient in solving both dispersion-dominated and advection-dominated transport problems (Baptista et al., 1984). They were successfully applied to simulate solute transport in drinking water distribution systems (Basha and Malaeb, 2007; Li, 2006; Tzatchkov et al., 2002). In the present model, a two stage Eularian-Lagrangian numerical scheme combined with the numerical Green's function technique proposed by Tzatchkov et al. (2002) is used. First, the Lagrangian step is executed using the explicit method of characteristics (MOCs) to solve the advection and reaction terms, then the Eularian step is executed to solve the dispersion term using an implicit finite difference scheme. The details of the employed Eularian-Lagrangian scheme are shown in the Supplementary material section S-1.

2.3. Stochastic demand generator

A stochastic model is developed in this study to simulate the behavior of flow demands in residential dead-ends that exhibit random temporal and spatial fluctuations. The model is connected to the dead end water quality simulator to provide the time variable flow demands at different withdrawal nodes. The model is developed based on the non-homogenous Poisson process that was introduced by Buchberger and Wu (1995) to simulate the stochastic intensity, duration and frequency of residential demands. Demand pulses are generated on instantaneous basis (i.e. second-by-second) as Poisson rectangular pulses arrive to consumption nodes at a non-homogenous arrival rate. Demand volumes are calculated as the summation of individual pulse volumes; that is the product of pulse intensity times duration. Flow rates are then averaged over a specified period known as pulse aggregation interval which was estimated to be 5 min in this study to sufficiently represent the potential effects of stochastic demands on model hydraulics and transport based on the results of Yang and Boccelli, 2014. Log-normal probability distributions were used to describe the intensity and duration of water pulses as Buchberger and Wells (1996) found that they provide favorable description of actual residential demands. The underlying equations used to develop the model are described by Buchberger and Li (2007) for the PRPSym model, and hence not shown here. Indoor and Outdoor water demands are generated as separate Poisson pulses and then aggregated to give the total instantaneous nodal demand. The statistical parameters used for both indoor and outdoor demand intensities and durations are taken from Nilsson et al. (2005).

2.4. Model application

The present model is first applied to simulate the concentrations of free chlorine and fluoride tracer in the dead end links of the Cherry Hills/Brushy Plains (CHBP) service area of the South Central Connecticut Regional Water Authority (SCCRWA). This residential network was previously used by Rossman et al. (1994) to compare the results of EPANET model with sampling data collected in the field campaign conducted by SCCRWA on August 13–15, 1991. The results of this specific campaign were later used by many researchers to verify water quality models in distribution systems (Basha and Malaeb, 2007; Tzatchkov et al., 2002; Yeh et al., 2008). The original study used a skeleton grid of the actual all-pipe CHBP network that has 32 dead ends. Sampling was conducted at the pump station and eight other locations through the network, two of which were on the terminal nodes of dead end links - Pipes 10 and 34 (Rossman et al., 1994). A list of the simulations performed using WUDESIM is given in Table 1, where eight different simulations were conducted to verify the model against field measurements, four Monte-Carlo ensembles were executed for the uncertainty analysis study, and 15 simulation scenarios were performed to test

Table 1
List of simulations performed.

A – Model verification simulations			
Simulation no.	Solute	Pipe no.	Axial hydraulic profile
1-A, B	Fluoride	10, 34	GA calibrated
2-A, B	Chlorine	10, 34	GA calibrated
3-A, B	Fluoride	10, 34	Equal shares
4-A, B	Chlorine	10, 34	Equal shares
B – Monte-Carlo simulations			
MC-Ensemble	Solute	Pipe no.	Demand variation
5-A	Fluoride	10	Spatial
5-B	Fluoride	10	Temporal
6-A	Chlorine	10	Spatial
6-B	Chlorine	10	Temporal
C – Sensitivity analysis simulations			
Simulation no.			Variation parameter
7			Base case
8-A, B			Flow rate
9-A, B			Pipe diameter
10-A, B			Pipe length
11-A, B			Average inlet concentration
12-A, B			Amplitude of inlet sine wave
13-A, B			Period of inlet sine wave
14-A, B			Bulk decay rate constant

the sensitivity of the model results to different input parameters.

3. Results and discussion

3.1. Model verification

As limited data was available on the residential neighborhood of the CHBP network, Google Earth® software was used to locate the two dead ends and identify the number of consumption points on each dead end through aerial photos captured on March 15, 1992 – approx. 7 months after the sampling study (See Section S-3.1). The axial locations of the withdrawal nodes were scaled from the aerial photos to be used in the simulation. Aerial photos (Fig. S-2) showed that pipes 10 and 34 could be simulated with seven and five consumption nodes, respectively, with axial spacing of at least 60 ft between each two consecutive nodes. This number was determined by counting the number of consumption points on each dead end assuming each building to represent a single consumption point. Consecutive buildings with a spacing less than 10% of the total dead end length were lumped into one consumption point.

The efficiency of any water quality simulator is greatly controlled by the proper calibration of the coupled hydraulic model. The individual water consumption of each withdrawal node on the dead end was unknown, unlike the lumped hourly demands which were available through Example 2 in EPANET as generalized demands. Hence, there was a need for a special technique to calibrate the time-averaged axial hydraulic profile in each of the two dead ends. Several techniques were previously developed for the calibration of hydraulic models in water distribution systems (Savic et al., 2009). Of these techniques, evolutionary optimization algorithms are conceptually simple as they do not involve complex mathematical procedures, yet they are robust and accurate in locating optimum solutions. Genetic algorithms (GAs) were used for hydraulic calibration in water distribution systems by few researchers (Gözütok and Özdemir, 2003; Lingireddy and Ormsbee, 1999). In the present study, genetic algorithms were used to calibrate the hydraulic model of the dead end by optimizing the share of each of the withdrawal nodes from the total pipe demand. The implemented fitness function represented the Coefficient of Variation of the root mean square deviation (RMSD) between field measured and simulated concentrations CV_{rms}:

$$Fitness = CV_{rms} = \frac{1}{\overline{C}_{meas}}\sqrt{\frac{\sum_{i=1}^{N_{meas}}(C_i - C_{sim})^2}{N_{meas}}} \tag{8}$$

Where, CV_{rms} is the deviation function targeted for minimization; C_i is the field measured concentration at some time t (mg/L); C_{sim} is the simulated concentration at time t (mg/L); N_{meas} is the number of field measurements; $\overline{C}_{meas}$ is the average overall field measured concentrations (mg/L). Fluoride tracer measurements were used for hydraulic calibration because the concentration of the non-reactive solute is only controlled by advection and dispersion. (Fig. 2) shows the simulation results of the present model for fluoride tracer in comparison with EPANET and ADRNET (Li, 2006) models plotted against field measurements. ADRNET is an ADR model that incorprates (Eq. (2)) as the governing equation. Both the present model and ADRNET use Eularian-Lagrangian numerical schemes and use stochastic flow demands generated based on Poisson processes. The reason for choosing ADRNET to compare with the model herein is to test the effect of considering spatial distribution of flow demands and transport parameters as well as the highly dynamic dispersion coefficient implemented herein. It is clear from the fluoride tracer results that advection based models such as EPANET are unable to efficiently simulate solute transport in dead-ends compared to advection-dispersion models, because

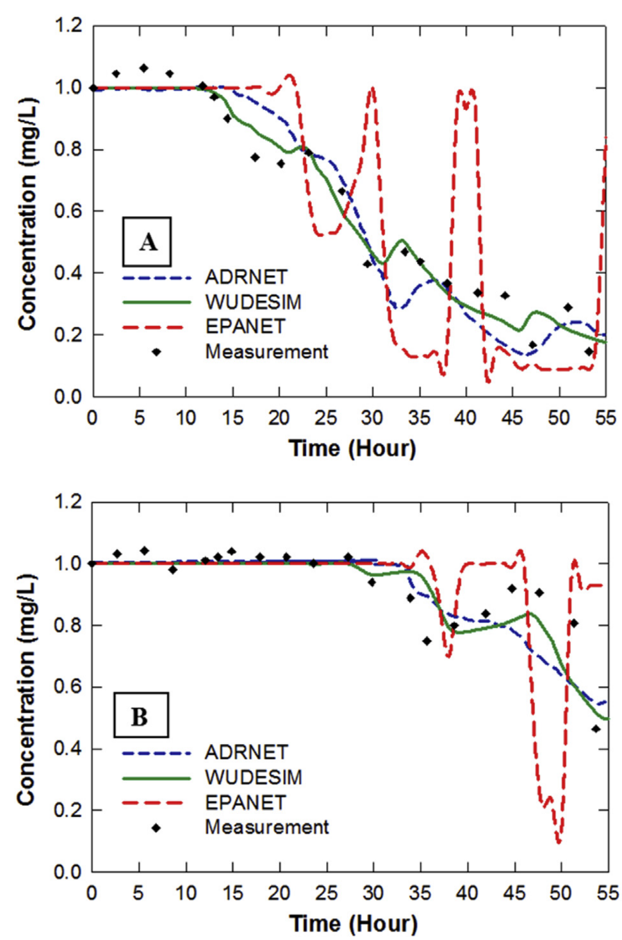

Fig. 2. Simulated outlet fluoride tracer concentrations using ADRNET model (Li, 2006), EPANET (Rossman et al., 1994) and WUDESIM (present model) against field measurements for: **(A)** Pipe 10; **(B)** Pipe 34.

the solute transport in dead-ends is mainly dispersion-dominated. Comparing the simulation results for WUDESIM with ADRNET, we found that our new model slightly better predicts field measurements due to the realistic consideration of flow velocity and dispersion coefficient. The optimized average hydraulic flow profile generated from GAs calibration of the shares of the withdrawal nodes indicated that the share of the last withdrawal node on both dead ends was noticeably larger than all other nodes in the optimized flow profile as it alone accounted for 35–40% of the total water volume consumed during the simulation period. Going back to the original sampling study presented by Clark et al. (1993), we found that a special fitting was installed on the hydrants where samples were collected to allow continuous flow of water at a rate ranging from 3.79 to 15.14 lpm (1–4 gpm). This could explain the reason why the terminal nodes had the largest demand share, and at the same time proved the efficiency of the implemented GA in optimizing the hydraulic profile.

(Fig. 3) shows the results for simulated concentrations of free chlorine by the three models plotted against field measurements. The values of the bulk and wall decay coefficients were taken as $k_b = 0.55$ day^{-1} and $k_w = 0.15$ m/day, matching the values previously used by EPANET and ADRNET. For both dead ends, the simulated concentrations by WUDESIM were in a remarkably better agreement with field measurements as illustrated by the CV_{rms} values shown in Table 2. The present model better simulates the excessive residence times in dead ends compared to ADRNET that

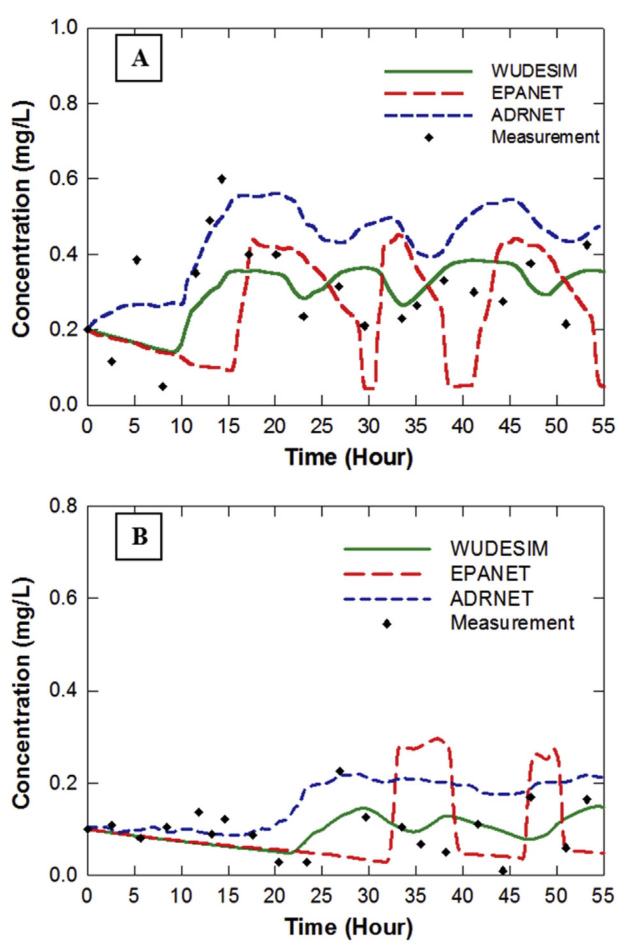

Fig. 3. Simulated outlet free chlorine concentrations using ADRNET model (Li, 2006), EPANET (Rossman et al., 1994), and WUDESIM (present model) against field measurements for: **(A)** Pipe 10; **(B)** Pipe 34.

tends to systematically overestimate the chlorine concentrations as spatial aggregation approximation under-simulates the residence time in dead ends. Chlorine disappearance in dead ends is mainly caused by long periods of stagnation usually encountered in the times of low demand. This also leads to excessive concentrations of disinfection by products DBPs in the extremities of the distribution network (Sadiq and Rodriguez, 2004).

The high degree of detail used herein to simulate dead end pipes represented by considering the exact axial locations of withdrawal points and the calibrated share of each node of the overall demand might not be available for water utilities in the design stage of the water distribution system. Hence, previous simulations were repeated but with considering equally spaced nodes with equal demand shares assuming the only known dead-end parameter is the number of withdrawal nodes. As shown in Table 2, simulation accuracy represented by the deviation function CV_{rms} dropped for all cases as a result of this approximation compared to the calibrated WUDESIM model. However, it still showed higher accuracy compared to both ADRNET and EPANET models especially for the case of chlorine, as the simulated residence time in the dead end is still closer to reality. The high magnitudes observed for the CV_{rms} in the case of chlorine are attributed to the unrealistic first order decay rate with a constant bulk decay coefficient which is inefficient in simulating bulk decay and should be replaced by a second order model (Clark, 1998), or more appropriately a dynamic reaction rate (Hua et al., 2015) which was out of the scope of the current study. Using the genetic algorithm to calibrate the wall demand k_w resulted in a slight enhancement in the simulation accuracy where the CV_{rms} dropped to 34.56% and 48.64% for pipe 10 and 34 respectively, using k_w values of 0.593 m/day and 0.3764 m/day respectively. The results showed minimal sensitivty to the variation of k_w as the bulk demand dominated chlorine decay due to relatively low flow velocities.

3.2. Computational efficiency

As the proposed modeling approach considers simulation of dead ends with a high level of spatial and temporal detail, this comes with an increased computational cost when compared to simple models with spatially aggregated, temporally averaged flow demands and steady dispersion rates. The added computational time takes place due to two main factors:

I. The extra computational step required to generate the stochastic flow demands aggregated at minor time steps that subsequently leads to an increased number of hydraulic steps for the total time of simulation. The computational time for this step increases as the required pulse aggregation time decreases where smaller water quality steps are required to capture flow variation at a higher level of temporal detail.
II. As the spatial variation in flow rates is considered, downstream pipe sections experience lower flow velocities, and hence finer discretization grids are generated for a particular water quality step (Eq. S.(3)). In addition, the multi-segment model introduces the need to solve an extra set of linear equations every quality step to generate the concentration at the connecting withdrawal nodes (Eq. S.(10)). The size of the system of equations increases as the number of considered sections increases.

To quantitatively illustrate the added computational burden, the proposed multi-segment modeling approach is used to simulate a typical residential dead end pipe of 244-m (800 ft) length and 20.3 cm (8-inch) nominal diameter. Five model simulations include a base flow rate of 600 L/hr in a diurnal water demand pattern (Fig. 4-a) for a 7 days period. The inlet chlorine concentration is

Table 2
CV_{rms} values (Eq. (8)) of different models.

Solute	WUDESIM		ADRNET (Li, 2006)	EPANET (Rossman et al., 1994)
	GA calibrated shares	Equal shares		
Fluoride				
Pipe 10	8.45%	13.69%	14.84%	33.49%
Pipe 34	8.14%	9.00%	9.26%	21.71%
Chlorine				
Pipe 10	36.66%	41.59%	54.22%	64.12%
Pipe 34	50.10%	51.90%	88.70%	101.10%

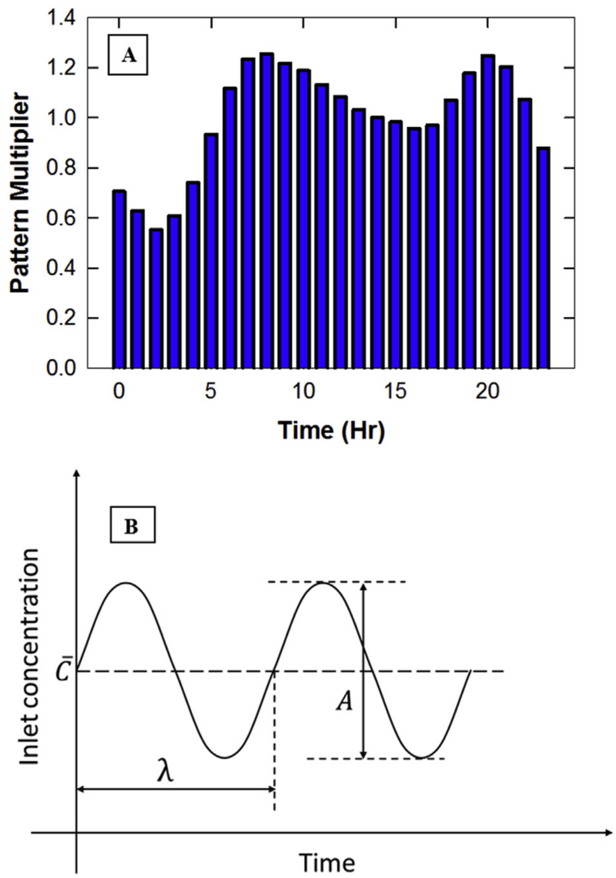

Fig. 4. **(A)** Demand pattern for base case scenario; **(B)** Time distribution of chlorine concentration at pipe inlet.

assumed to have a sinusoidal time distribution (Fig. 4-b) given by: $C_0(t) = \overline{C}_0 + A * \sin\left(\frac{2\pi t}{\lambda}\right)$, where $\overline{C}_0 = 10$ mg/L, $A = 2.5$ mg/L and $\lambda = 6$ h. The choice of the sinusoidal time distribution was based on the study of (Li et al., 2005) where the results showed that axial dispersion plays a key role in solute transport for the cases of instantaneous and sinusoidal profiles of solute source. A bulk and wall decay rates are 0.5 day^{-1} and 0.5 m/day, respectively. Under these conditions, the first simulation using the simplified ADR model takes the dead end as a single segment pipe with hourly flow demands lumped at the outlet and a steady Taylor's dispersion coefficient representing a simplified model. For the other four simulations, the stochastic demand generator was used to produce demand pulses aggregated at a 5 min period with each simulation considering a different number of sections or homes (5, 10, 15 and 20 respectively). They represent the detailed modeling approach using dynamic dispersion coefficients as proposed by the current study. The differences in model setup between the simplified and the detailed models are summarized in Table 3. All five simulations were performed on a personal computer equipped with an Intel®-Core™i7 3632QM CPU @2.2 GHz capable of performing 70.4 GFLOPS – peak theoretical performance. The software environment used to perform the simulations was MATLAB R2013a while the genetic algorithm simulations were performed using the associated Optimization Toolbox 6.3. As shown in (Fig. 5), the required CPU time for the 5 segment model is almost 10 times as big as the simplified model. The CPU time then increases linearly with the number of sections considered by the model.

3.3. Sensitivity analysis

From a practical point of view, a typical water distribution system comprises several hundred dead end links. This complexity leads to massive computational requirement, making it very difficult to use such a sophisticated model in real time to account for all network dead ends. Thus we conducted a parametric sensitivity analysis to help decide when to use the simplified single segment model vs. the proposed detailed model. The objective was to understand how the two models differ under the variation of different simulation parameters that were classified into three groups: (i) hydraulic parameters, (ii) pipe specific parameters, and (iii) solute specific parameters. The values for the variable parameters are shown in Table 4.

The base case scenario represents the same parameters as in the computational time analysis. Then, one parameter is changed at a time from the base case, resulting in a total of 15 different scenarios. All five simulations described previously are repeated for each scenario for the simplified model and for the detailed model with 5, 10, 15 and 20 segments/homes. The deviation in model outputs was evaluated as the CV_{rms} (Eq. (8)) of the outlet concentrations between the two models. This deviation reflected the error generated by the simplified model compared to the detailed model, assuming detailed model to be exact. The results show that the deviation scales up as the number of segments increases because the error due to the spatial aggregation approximation increases with the number of withdrawal points on the dead end pipe. The results showed that the CV_{rms} strongly depends on four out of the seven studied parameters, where the increase of the pipe diameter, pipe length, and bulk decay coefficient, and the decrease of the base flow rate all resulted in an increase of the CV_{rms}. Parameters controlling the time distribution of inlet concentration profile showed negligible influence on the deviation between the simplified and the detailed models.

To generalize the findings on the effect of different individual parameters, a set of three dimensionless parameters was evaluated for each scenario: the Reynolds number (*Re*), axial Peclet number (*Pe*) and the Damkohler number (*Da*). They were calculated as a time-average value for the single segment case in each simulation scenario.

As shown in (Fig. 6-a, & b), the CV_{rms} dropped as the simulation Reynolds number increased, but increased with the increase in the

Table 3
Summary of the differences between the simplified and the detailed model.

Parameter	Simplified model	Detailed model
Demand distribution		
Spatial	Aggregated (single segment)	Multiple segments
Temporal	Averaged (hourly basis)	Stochastic demand pulses
Dispersion rate	Steady Taylor's dispersion (Eq. (4))	Dynamic (Eq. (5))

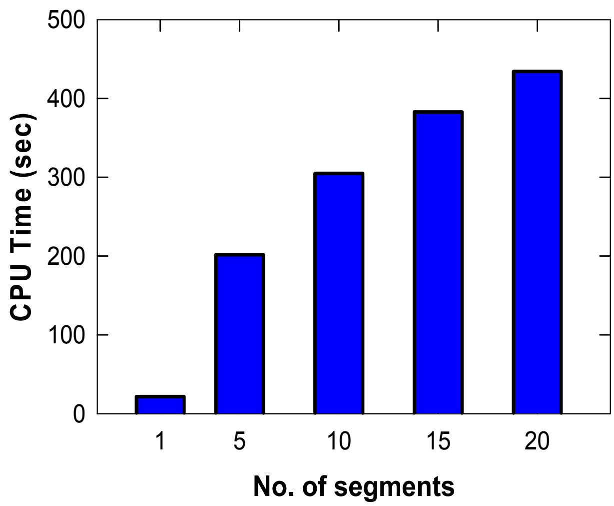

Fig. 5. Simulation time for base case scenario as a function of the number of segments.

leading to an overall smaller Damkohler number.

3.4. Uncertainty analysis

Residential water demands exhibit large temporal and spatial fluctuations; both directly affect the disinfectant transport and reaction in the distribution network. A Monte-Carlo simulation approach was implemented to understand the extent to which spatial distribution and temporal variation of water demands affect the efficacy of the simulation model in predicting disinfectant residuals in dead ends.

Statistical parameters are typically used to simulate residential demand pulses, where wide disparities generally exist in the intensity, duration and frequency of outdoor demand pulses compared to indoor demand pulses (Lee and Buchberger, 2004). Thus the generated time series of aggregated flows heavily depend on the ratio of indoor/outdoor demands to the total flow demand (See Fig. S-5). In this study, the average and standard deviation for the intensity of indoor demand pulses were taken as 8.52 lpm and 4.73 lpm respectively. For outdoor demand pulses, these values increased to 15.14 lpm and 3.79 lpm, respectively. The uncertainty in temporal distribution of flow demands was considered by taking the percentage of indoor demands out of the total nodal demand to be uncertain. The uncertainty in the spatial distribution of flow demands was studied by considering the share of each withdrawal point from a fixed total pipe demand for the dead end to be the uncertain parameter. Thus four sets of Monte-Carlo ensembles were executed where each set comprised 200 individual simulations (Table 1). All simulations were conducted to the dead end pipe 10 in the CHBP study which has seven withdrawal nodes as aforementioned. The first two sets (5-A, B) are intended to compare the uncertainty in the predicted conservative tracer (fluoride) concentration profile due to temporal heterogeneity versus spatial heterogeneity. The other two sets (6-A, B) investigated the uncertainty in the concentration of a reactive disinfectant (free chlorine).

To isolate the two different sources of uncertainty, the time distribution of the total pipe demand was kept unchanged for all spatial variation simulations. The share of each withdrawal node was assumed to follow a lognormal distribution with an average of ($1/N_{seg}$), where N_{seg} is the number of considered pipe segments ($N_{seg} = 7$ for pipe 10), and a standard deviation of the same magnitude. Similarly for the temporal variation simulations, all

Table 4
Simulation parameter values for the sensitivity analysis study scenarios.

Parameter		Min	Base case	Max
(i) Hydraulic	Q_b (L/hr)	300	600	900
(ii) Pipe specific	d (cm)	15.24 [6″]	20.32 [8″]	25.40 [10″]
	L (m)	121.92 [400′]	243.84 [800′]	365.76 [1200′]
(iii) Solute specific	$\overline{C}_0$ (mg/L)	5	10	15
	A (mg/L)	1	2.5	4
	λ (hr)	3	6	9
	k_b (day^{-1})	0.05	0.5	1.5

Peclet number. This shows that the average flow velocity has a critical influence on the error in the simplified model, whereas the error drops rapidly as the flow velocity increases. Although by definition the axial Peclet number is directly proportional to the flow velocity, the dispersion coefficient in the denominator is a function of (u^2) based on Taylor's definition given by Eq. (4). Thus the overall dependence of Peclet number is inversely proportional to the flow velocity, or more specifically, directly proportional to the characteristic residence time: $\tau_0 = L/u$. It can also be seen from (Fig. 6-a) that the effect of Reynolds number fades as the flow approaches the upper bounds of laminar regime for the 5 segments pipe scenario, a consequence that was expected as the advective transport becomes mainly dominant and the role of dynamic dispersion diminishes in comparison with the steady Taylor dispersion. From (Fig. 6-c), it's clear that with an increase in Damkohler number, the CV_{rms} scales up. This further shows that the increase in the flow velocity or the drop in the characteristic residence time will reduce the error associated with the simplified model. The flow velocity plays an interesting role in this particular case, because the increase of the flow velocity also enhances mass transfer of disinfectants to the pipe wall or k_f, and thus the calculated overall first-order decay constant in (Eq. (2)). However, increasing the flow velocity decreases the residence time sharply

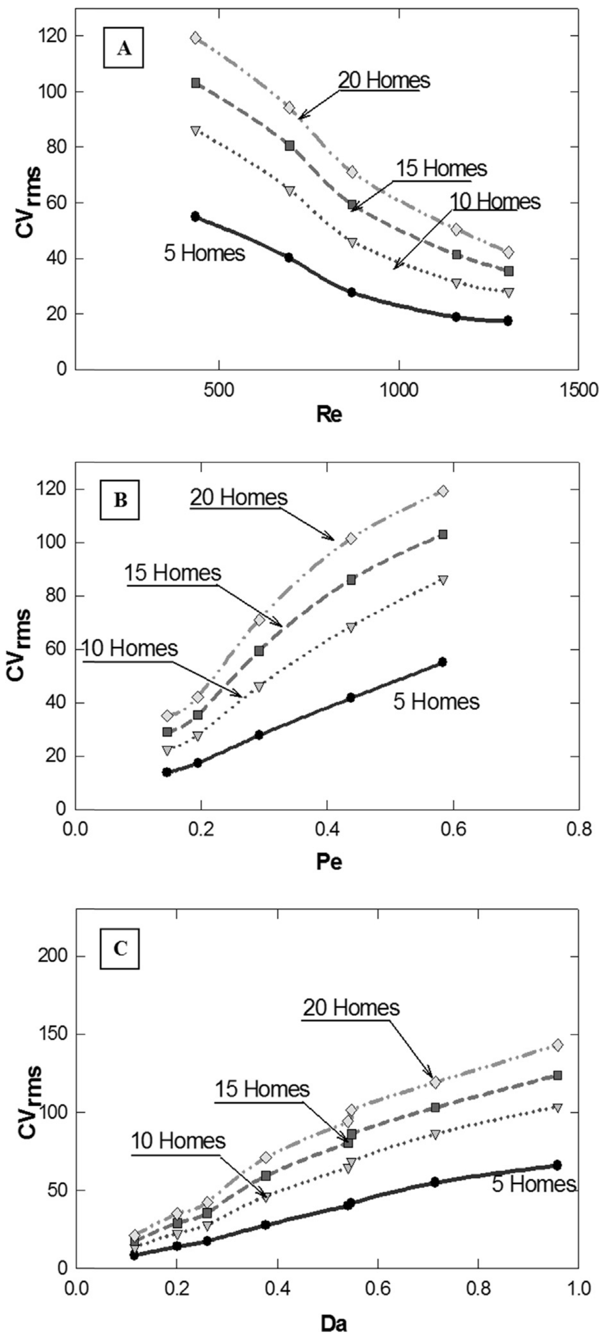

Fig. 6. (A)–(C) dependence of the CV_{rms} on the time averaged Reynolds number (*Re*), Peclet number (*Pe*) and Damkohler number (*Da*), respectively.

withdrawal points were assigned equal shares of the total pipe demand. The indoor demands ratio was given a uniform probability distribution with a minimum of 50% and maximum of 100%. To insure the convergence of the simulated 200 realizations, the average and standard deviation of the simulation RMSD were calculated after each realization until reaching a stable value. All four Monte-Carlo simulations converged relatively quickly (<100 simulations).

The analysis results showed that the uncertainty in the generated concentration profile due to variability in the spatial distribution of water demands was significantly larger than that caused by temporal variability. This conclusion applies for both conservative tracer and reactive disinfectant cases. (Fig. 7-a, & b) shows the time evolution for the coefficient of variation in the outlet concentration-time profiles for the four Monte-Carlo simulation ensembles. The uncertainty in the fluoride concentration profile was consistently larger than that of the reactive free chlorine for both temporal and spatial variability simulations. This effect suggests that the decay term in (Eq. (2)) attenuates the difference between simulation results of hydraulic dispersion under different flow demand distributions. Another factor that showed great dependence on the spatial demand distribution compared to temporal distribution was the simulation accuracy. (Fig. 7-c, & d) shows the Box-and-Whisker plots of the distribution of the CV_{rms} values of the four Monte-Carlo ensembles. While temporal variation showed minimal effect on the simulation accuracy, spatial distribution showed significant influence for both cases of fluoride tracer and free chlorine. It is also clear that the variation in the CV_{rms} values for the case of free chlorine is minor compared to fluoride tracer which is consistent with the uncertainty analysis results.

4. Correction factors for spatial aggregation

Temporal distribution of flow demands was shown in the uncertainty analysis to have minimal effect on the solute transport compared to the spatial distribution. In the sensitivity analysis, we further showed that the spatial aggregation in water demand is the primary source of modeling errors using the simplified model as compared to the detailed model. These modeling and analysis results suggest that the temporal averaging assumption represented by the implementation of hourly averaged flow rates and steady dispersion coefficients will not significantly compromise the accuracy, while spatial aggregation would. However, using multi-segment model to simulate the dead end was shown to greatly increase the computational cost compared to the simplified model.

Therefore to approximate the behavior of the detailed model and reduce computational demand, we have proposed a set of three correction factors analytically derived for the simplified model when the number of withdrawal points is known for a dead end pipe. The correction factors were developed in a way that translates the three dimensionless groups *Re*, *Pe* and *Da* from a multi-segment to a single-segment model while using hourly averaged demands and steady dispersion rates. The detailed derivation is given in the Supplementary material Section (S-2). The correction factors for the residence time CF_τ, Taylor's dispersion coefficient CF_E, and the overall wall demand CF_R are:

$$CF_\tau = \frac{\tau_{corr}}{\tau_0} = \sum_{i=1}^{N_{seg}} \frac{1}{N_{seg} - i + 1} \tag{9}$$

$$CF_E = \frac{E_{T,corr}}{E_{T,0}} = \frac{\sum_{i=1}^{N_{seg}} (N_{seg} - i + 1)^2}{N_{seg}^3} \tag{10}$$

$$CF_R = \frac{R_{w,corr}}{R_{w,0}} = \frac{1}{CF_\tau} \sum_{i=1}^{N_{seg}} (N_{seg} - i + 1)^{-2/3} \tag{11}$$

The 15 different scenarios considered in the sensitivity analysis study were re-simulated after applying the correction factors to the simplified model. The CV_{rms} was plotted before and after applying the corrections for the cases of 5, 10, 15 and 20 segments. Obviously in (Fig. 8), the correction factors greatly enhanced the simulation accuracy where the error dropped for all the simulated scenarios. The enhancement of the accuracy increased with increasing pipe diameter, pipe length and bulk decay coefficient, and decreasing the flow rate. This result again affirms the role of the residence time as the main controlling parameter, and the increased effectiveness

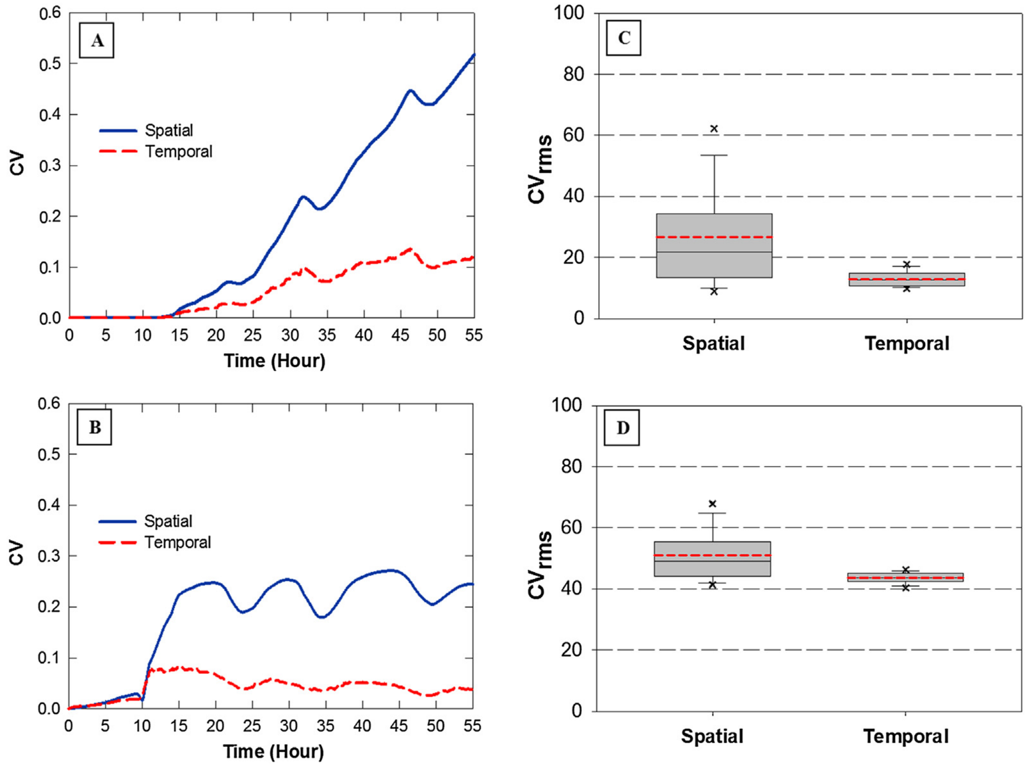

Fig. 7. **(A)** & **(B)**: Time evolution of the coefficient of variation *CV* for the concentration profiles of fluoride tracer and free chlorine respectively; **(C)** & **(D)**: Box-and-Whisker plots of the CV_{rms} of fluoride tracer and free chlorine respectively. Tick marks represent the 5th/95th percentile rang.

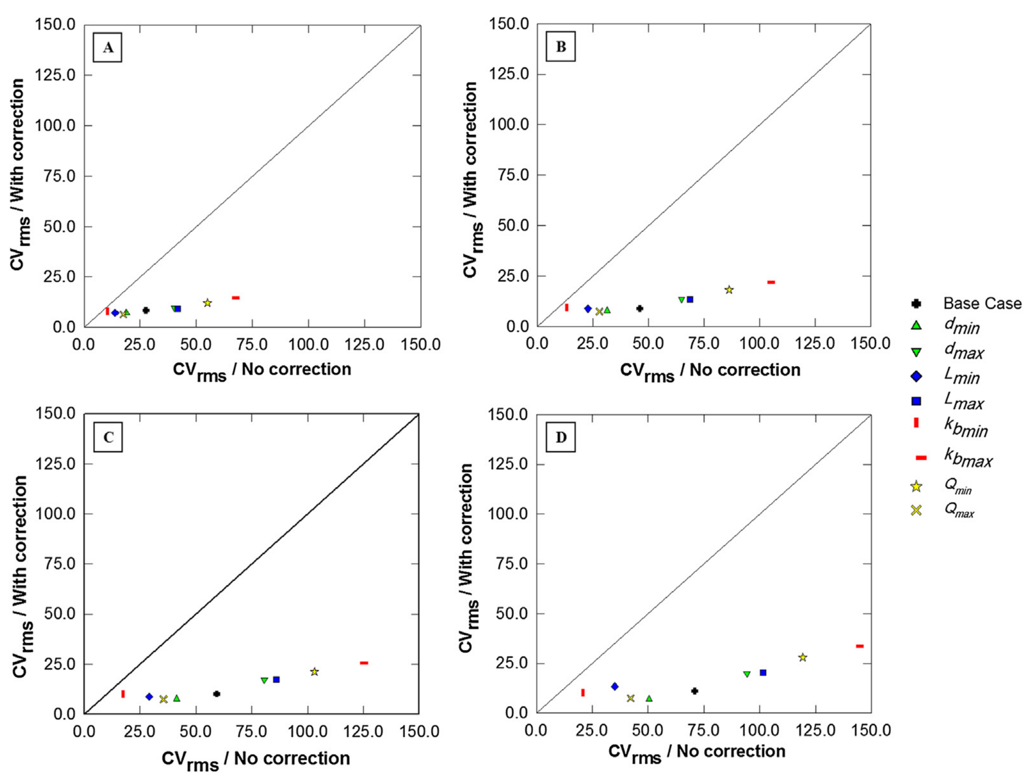

Fig. 8. Comparison of the CV_{rms} before and after applying the derived correction factors. (A)–(D) represent the 5, 10, 15 and 20 segments scenarios, respectively.

of the correction factors at higher residence time in the pipe.

5. Conclusions

A numerical model, WUDESIM, was developed to simulate disinfectant residuals in the dead end mains of water distribution systems. This is so far the first study to account for the combined effects of spatial and temporal distribution of flow demands on disinfectant transport in dead ends. The model represents the spatial distribution of flow demands by considering multiple draw-off nodes that withdraw water and disinfectant along the axis of the pipe. Temporal distribution of demand pulses was simulated using a non-homogenous Poisson process. The model implemented highly dynamic dispersion rates for pulsating laminar flows, and employed an Eularian-Lagrangian numerical scheme to solve the 1-D advection-dispersion-reaction equation. A genetic algorithm optimization technique was used to calibrate the hydraulic profile of the dead-end. A Monte-Carlo simulation was executed to investigate the influence of spatial and temporal distributions of flow demands on the simulation accuracy.

The simulation results of the new model showed better agreement with field measured concentrations when compared to an advection based model EPANET as well as an advection-dispersion based model ADRNET. Analysis of the results suggest that spatial distribution of flow demands have significant influence on the generated concentration profile, and subsequently, the simulation accuracy. The approximation of spatial aggregation of flow demands should be avoided in simulating water quality in the dead ends because it might substantially reduce the simulation accuracy. Water quality models treating dead-end pipes as multiple segments with spatially variable hydraulic and transport parameters can yield more realistic residence times and disinfectant concentrations.

Acknowledgments

This work was partially funded by U.S. EPA through the CB&I Contract EP-C-4-014. The research described herein has been subjected to the Agency's peer and administrative review and has been approved for external publication. Any opinions expressed in this paper are those of the authors and do not necessarily reflect the views of the Agency, therefore, no official endorsement should be inferred. Any mention of trade names or commercial products does not constitute endorsement or recommendation for use. The authors would like to thank Dr. Ravindra Gudi for providing valuable comments on the article.

Appendix A. Supplementary data

Supplementary data related to this article can be found at http://dx.doi.org/10.1016/j.watres.2015.11.025.

References

Axworthy, D.H., Karney, B.W., 1996. Modeling low velocity high dispersion flow in water distribution systems. J. Water Resour. Plan. Manag. 122 (3), 218–221.

Baptista, A.E., de M., Adams, E.E., Stolzenbach, K.D., 1984. Eulerian-lagrangian Analysis of Pollutant Transport in Shallow Water. Energy Lab. Massachusetts Inst. Technol, Cambridge, Mass. Rep. No. MIT-EL 84–008.

Barbeau, B., Gauthier, V., Julienne, K., Carriere, A., 2005. Dead-end flushing of a distribution system: short and long-term effects on water quality. Aqua J. Water Supply Res. Technol. 54 (6), 371–383.

Basha, H.A., Malaeb, L.N., 2007. Eulerian–Lagrangian method for constituent transport in water distribution networks. J. Hydraul. Eng. 133 (10), 1155–1166.

Biswas, P., Lu, C., Clark, R.M., 1993. A model for chlorine concentration decay in pipes. Water Res. 27 (12), 1715–1724.

Buchberger, S.G., Lee, Y., 1999. Evidence supporting the poisson pulse hypothesis for residential water demands. In: Proc. CCWI Int. Conf. Comput. Control Water Ind.

Buchberger, S.G., Li, Z., 2007. PRPsym: a modeling system for simulation of stochastic water demands. In: World Environ. Water Resour. Congr, pp. 1–13. http://dx.doi.org/10.1061/40927(243)511.

Buchberger, S.G., Wells, G.J., 1996. Intensity, duration, and frequency of residential water demands. J. Water Resour. Plann. Manag. 122 (1), 11–19.

Buchberger, S.G., Wu, L., 1995. Model for instantaneous residential water demands. J. Hydraul. Eng. 121 (3), 232–246.

Clark, R.M., 1998. Chlorine demand and TTHM formation kinetics: a second-order model. J. Environ. Eng. 124 (1), 16–24.

Clark, R.M., Grayman, W.M., Males, R.M., Hess, A.F., 1993. Modeling contaminant propagation in drinking-water distribution systems. J. Environ. Eng. 119 (2), 349–364.

Ekambara, K., Joshi, J.B., 2003. Axial mixing in pipe flows: turbulent and transition regions. Chem. Eng. Sci. 58, 2715–2724. http://dx.doi.org/10.1016/S0009-2509(03)00102-7.

Galvin, R., 2011. Eliminate dead-end water. OPFLOW – AWWA Mag. 37 (11), 20–21.

Gözütok, S., Özdemir, O.N., 2003. Refinement of hydraulic calibration for water supply networks with genetic algorithms. In: World Water Environ. Resour. Congr, pp. 1–7. http://dx.doi.org/10.1061/40685(2003)131.

Grayman, W.M., 2006. A quarter of a century of water quality modeling in distribution systems. In: Water Distrib. Syst. Anal. Symp. Cincinnati, Ohio, USA, pp. 1–12. http://dx.doi.org/10.1061/40941(247)4.

Hua, P., Vasyukova, E., Uhl, W., 2015. A variable reaction rate model for chlorine decay in drinking water due to the reaction with dissolved organic matter. Water Res. 75, 109–122. http://dx.doi.org/10.1016/j.watres.2015.01.037.

Islam, M.R., Chaudhry, M.H., 1998. Modeling of constituent transport in unsteady flows in pipe networks. J. Hydraul. Eng. 124 (11), 1115–1124.

Lee, Y., 2004. Mass Dispersion in Intermittent Laminar Flow (PhD Diss). Univ. Cincinnati, Cincinnati, Ohio, USA.

Lee, Y., Buchberger, S.G., 2004. Modeling indoor and outdoor residential water use as the superposition of two poisson rectangular pulse processes. Methodology. http://dx.doi.org/10.1061/40430(1999)48.

Li, Z., 2006. Network Water Quality Modeling with Stochastic Water Demands and Mass Dispersion. University of Cincinnati, Cincinnati, Ohio, USA (PhD Dissertation).

Li, Z., Buchberger, S.G., Tzatchkov, V., 2005. Importance of dispersion in network water quality modeling. Impacts Glob. Clim. Chang. 1–12. http://dx.doi.org/10.1061/40792(173)27.

Li, Z., Buchberger, S.G., Tzatchkov, V., 2006. Integrating distribution network models with stochastic water demands and mass dispersion. In: Water Distrib. Syst. Anal. Symp. Cincinnati, Ohio, USA, pp. 1–15.

Lingireddy, S., Ormsbee, L.E., 1999. Optimal network calibration model based on genetic algorithms. In: 29th Annu. Water Resour. Plan. Manag. Conf. Tempe, Arizona, United States, pp. 1–8.

Nilsson, K.A., Buchberger, S.G., Clark, R.M., 2005. Simulating exposures to deliberate intrusions into water distribution systems. J. Water Resour. Plan. Manag. 131 (3), 228–237.

Ozdemir, O.N., Ger, A.M., 1998. Realistic numerical simulation of chlorine decay in pipes. Water Res. 32 (11), 3307–3312.

Ozdemir, O.N., Ger, A.M., 1999. Unsteady 2-d chlorine transport in water supply pipes. Water Res. 33 (17), 3637–3645.

Ozdemir, O.N., Ucak, A., 2002. Simulation of chlorine decay in drinking-water distribution systems. J. Environ. Eng. 128 (1), 31–39.

Rossman, L.A., 2000. Epanet 2-User's manual. United States Environ. Prot. Agency (EPA), Cincinnati, OH.

Rossman, L.A., Clark, R.M., Grayman, W.M., 1994. Modeling chlorine residuals in drinking-water distribution systems. J. Environ. Eng. 120 (4), 803–820.

Sadiq, R., Rodriguez, M.J., 2004. Disinfection by-products (DBPs) in drinking water and predictive models for their occurrence: a review. Sci. Total Environ. 321, 21–46. http://dx.doi.org/10.1016/j.scitotenv.2003.05.001.

Sattar, A., 2013. Gene expression models for the prediction of longitudinal dispersion coefficients in transitional and turbulent pipe flow. J. Pipeline Syst. Eng. Pract. 5, 4013011. http://dx.doi.org/10.1061/(ASCE)PS.1949-1204.0000153.

Savic, D.A., Kapelan, Z.S., Jonkergouw, P.M.R., 2009. Quo vadis water distribution model calibration? Urban Water J. 6 (1), 3–22. http://dx.doi.org/10.1080/15730620802613380.

Taylor, G., 1953. Dispersion of soluble matter in solvent flowing slowly through a tube. Proc. Roy. Soc. London Ser. A, London, U.K. 219 (1137), 186–203.

Taylor, G., 1954. The dispersion of matter in turbulent flow through a pipe. Proc. Roy. Soc. London Ser. A, London, U.K. 223 (1155), 446–468.

Tzatchkov, V.G., Aldama, A.A., Arreguin, F.I., 2002. Advection-dispersion-reaction modeling in water distribution networks. J. Water Resour. Plan. Manag. 128 (5), 334–342.

Van Genuchten, M.T., Alves, W.J., 1982. Analytical Solutions of the One-dimensional Convection-dispersive Solute Transport Equation. U.S. Dept. Agric, Washington, D.C. Tech. Bull. No. 1661.

Yang, X., Boccelli, D.L., 2014. Simulation study to evaluate temporal aggregation and variability of stochastic water demands on distribution system hydraulics and transport. J. Water Resour. Plan. Manag. 140, 04014017. http://dx.doi.org/10.1061/(ASCE)WR.1943-5452.0000359.

Yeh, H.-D., Wen, S.-B., Chang, Y.-C., Lu, C.-S., 2008. A new approximate solution for chlorine concentration decay in pipes. Water Res. 42, 2787–2795. http://dx.doi.org/10.1016/j.watres.2008.02.012.